

# Elucidating the Biophysical Processes Responsible for the Chromatic Attributes of Peripheral Cyanosis

Gladimir V. G. Baranoski<sup>1</sup>, Senior Member, IEEE, Spencer R. Van Leeuwen<sup>1</sup> and Tenn F. Chen<sup>2</sup>

**Abstract**—The purple or blue coloration of hands and feet, known as peripheral cyanosis, can represent one of the initial signs of potentially life threatening medical conditions. Consequently, procedures aimed at its early detection and interpretation can help health-care professionals to select the appropriate treatment for these conditions. The effectiveness of such procedures, in turn, depends on the correct assessment of the biophysical processes responsible for eliciting this abnormal skin appearance. However, despite the diverse body of existing clinical research involving cyanosis, the interplay between physiological changes and the optical phenomena leading to cyanotic responses remains not fully understood. In this paper, we methodically examine this interplay through controlled *in silico* experiments. Among other relevant aspects, the results of our experiments demonstrate that Rayleigh scattering, a light attenuation phenomenon overlooked by previous studies on peripheral cyanosis, plays a pivotal role in the manifestation of cyanotic chromatic attributes. We believe that the insights derived from our experiments can contribute to the development of more effective protocols for the screening of medical conditions associated with peripheral cyanosis etiology.

**Index Terms**—cyanosis, hemoglobin, skin, fingertip, vein, reflectance, light attenuation, Rayleigh scattering, simulation.

## I. INTRODUCTION

Cyanosis refers to the purple or blue coloration of nail beds, skin and mucosal membranes (*e.g.*, lips and tongue) prompted by the presence of high levels of deoxygenated hemoglobin (deoxyhemoglobin) in the dermal tissues [1], [2]. It can be classified as being either peripheral or central [1], [3], [4]. Peripheral cyanosis is more apparent on the extremities (hands and feet), and it is more likely to occur when oxygen demand exceeds supply in these tissues [2], [3], [4]. This may result from peripheral circulatory failure (*e.g.*, due to reduced cardiac output), peripheral vasoconstriction (*e.g.*, due to hypothermia) or peripheral vascular occlusion (*e.g.*, due to arterial thrombosis) [1], [3], [4]. Central cyanosis, on the other hand, results from systemic hypoxemia (abnormally low level of oxygen in the blood), and it is also visible in the mucosal membranes in addition to the extremities [1], [3]. It is worth noting that both forms of cyanosis may be prompted by the presence of abnormal amounts of dysfunctional hemoglobins, namely



Fig. 1. Photographs depicting the palmar surfaces of two hands exhibiting normal (left) and cyanotic (right) skin appearances. The latter is a courtesy of James Heilman, MD.

methemoglobin (MetHb), sulfhemoglobin (SulfHb) or carboxyhemoglobin (CarboxyHb), in the dermal tissues [3], [4], [5]. However, this type of cyanosis-triggering situation is relatively rare [6], particularly when compared to those associated with the presence of high levels of deoxyhemoglobin.

Although it has been long recognized that dermal blood content [7] and oxygen saturation [8] play important roles in the manifestation of peripheral cyanotic chromatic attributes, to the best of our knowledge, no attempt has been made to date to systematically analyze their combined impact on these attributes. In this paper, we present the results of controlled experiments aimed at this objective.

Our investigation is focused on peripheral cyanosis for the following reasons. First, it usually shows up earlier [3], particularly in areas of the body characterized by low levels of melanin and relatively abundant blood supply such as palmar surfaces (Fig. 1). Central cyanosis, on the other hand, is generally a late finding in the course of a illness [4]. Second, all factors responsible for central cyanosis can also result in peripheral cyanosis [4]. Third, it may represent the initial sign of a catastrophic illness such as heart failure due to coronary occlusion, which can ultimately lead to myocardial infarction (heart attack) [1], [3], [4].

From an optical point of view, peripheral cyanotic chromatic attributes have been often associated with the light absorption properties of deoxyhemoglobin, with several authors incorrectly attributing the typical cyanotic bluish hue to an allegedly blue appearance of deoxygenated blood (*e.g.*, [1], [3], [4], [9], [10]). However, one has to consider the fact that the hemoglobins are strong absorbers in the “blue” end (400 to 500 nm) of the visible spectrum (Fig. 2 (left)). In addition, light traveling within the skin tissues is also strongly attenuated by the melanins, which are also strong absorbers in this spectral region (Fig. 2 (right)). Consequently, arterial blood appears bright red, while venous blood appears dark red,

\*This work was supported in part by the Natural Sciences and Research Council of Canada (NSERC) under Grant 238337.

<sup>1</sup> Gladimir V. G. Baranoski and Spencer Van Leeuwen are with the Natural Phenomena Simulation Group, School of Computer Science, University of Waterloo, 200 University Avenue, Waterloo, Ontario, N2L 3G1, Canada. gvgbaran@cs.uwaterloo.ca

<sup>2</sup> Tenn F. Chen is with Google Inc., 1600 Amphitheatre Pkwy, Mountain View, CA 94043, USA.

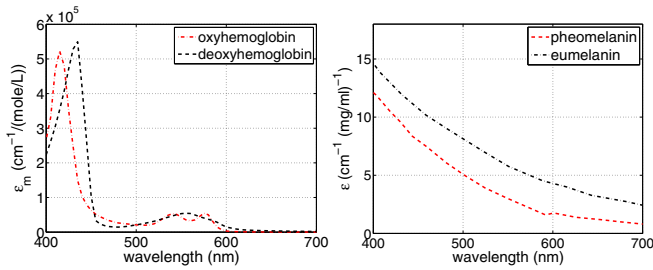


Fig. 2. Absorption spectra of functional hemoglobins (left) and melanins (right) found in the skin tissues. The former is provided in terms of molar extinction coefficient ( $\epsilon_m$ ) curves [15], while the latter is provided in terms of extinction coefficient ( $\epsilon$ ) curves [16].

almost black, but not blue [11], [12]. Hence, the purple or blue coloration of cyanotic skin must be also associated with other light attenuation phenomena besides the absorption by pigments like the hemoglobins.

It has been suggested [13] that thin connective structures, such as those found in the papillary dermis, can attenuate light through Rayleigh scattering. We believe that this phenomenon, which predominantly affects light propagating at lower wavelengths [14], has a pivotal part in the manifestation of typical cyanotic purple and blue hues. Accordingly, in this paper, we also present the results of controlled experiments aimed at the assessment of this hypothesis.

## II. INVESTIGATION FRAMEWORK

Predictive computer simulations, or *in silico* experiments, are often employed in biomedical research to accelerate hypothesis generation and validation cycles, particularly when it involves biophysical processes that cannot be fully studied through “wet” laboratory procedures due to logistic limitations [17], [18]. Among these limitations, one can highlight the relative scarcity of test cases, which may not be practical or safe to educe on live subjects (*e.g.*, [19]), and the relative large number of biophysical variables that need to be kept fixed during the procedures (*e.g.*, [6], [18]).

Following this trend, the investigation presented in this paper makes use of controlled *in silico* experiments to overcome such limitations. These experiments were performed using a first-principles light transport model for human skin, known as HyLloS (*Hyperspectral Light Impingement on Skin*) [20], and biophysical data provided in the scientific literature. More specifically, we employed HyLloS to compute directional-hemispherical reflectance curves for a selected skin specimen subjected to different peripheral cyanosis-triggering conditions.

It important to note that the predictive capabilities of the HyLloS model have been extensively evaluated through quantitative and qualitative comparisons of its outcomes with actual measured data [20]. Since then, this model has been reliably employed in a number of related biomedical investigations (*e.g.*, [18], [21], [22], [23]).

Within the HyLloS’ geometrical-optics formulation, light interacting with a given skin specimen is represented by rays that can be associated with any wavelength. Hence, this model can provide reflectance curves with different spectral

resolutions. For consistency, all modeled curves depicted in this work have a spectral resolution of 5 nm. These were obtained using a virtual spectrophotometer [24]. In their computation, we considered an angle of incidence of 10° and 10<sup>6</sup> sample rays.

To enable the full reproduction of our *in silico* experimental results, we made HyLloS available online [25] via a model distribution system [26]. This system enables researchers to specify experimental conditions (*e.g.*, angle of incidence and spectral range) and specimen characterization parameters (*e.g.*, pigments and water content) using a web interface [25], and receive customized simulation results. In addition, the supporting data (*e.g.*, refractive index and extinction coefficient curves) used in our investigation are also available online [27].

The noninvasive measurement of blood related properties (*e.g.*, oxygen saturation levels [2]) is usually performed at hypopigmented sites, such as the palmar fingertips, characterized by a reduced melanin content (more than five-fold lower than in the nonpalmoplantar regions [28]) and increased blood content [29]. As mentioned earlier, these characteristics also make these sites more susceptible to chromatic variations associated with peripheral cyanosis. For these reasons, we have elected the palmar fingertip as the testing site for our *in silico* experiments.

Without loss of generality, we have characterized a fingertip specimen in its normal (baseline) state using the dataset presented in Table I. The selection of values for this dataset parameters was based on physiologically valid ranges provided in related references, which are also listed in Table I. We note that, for some of these parameters, the selection of values within physiologically valid ranges required the use of multiple supporting references. In these instances, to conserve space, we cited one of our previous related publications [18] in which the interested reader can find the complete bibliographic information about these supporting references.

We employed the dataset provided in Table I to compute the baseline reflectance curve (depicted in Fig. 3 (top right)), and modified versions of this dataset to compute the remaining reflectance curves (depicted in Figs. 4 and 6) associated with the two sets of *in silico* experiments described in this paper.

In our first set of experiments, we investigated the combined impact of the dermal oxygenation fraction (given in %) and the reticular dermis blood content (given in % and denoted by  $v_{blood}^{rd}$ ) on the manifestation of peripheral cyanotic chromatic attributes. Note that the former parameter can be represented by  $100 - f_{deoxy}$ , where  $f_{deoxy}$  (given in %) indicates the fraction of deoxyhemoglobin to the total amount of functional hemoglobins present in the dermal tissues. Thus, we computed reflectance curves for the fingertip specimen considering  $f_{deoxy}$  variations from 25% to 100% and  $v_{blood}^{rd}$  variations from 5% to 20% [30].

In our second set of experiments, we investigated the connection between the peripheral cyanotic chromatic attributes and the putative occurrence of Rayleigh scattering within the

TABLE I

PARAMETERS EMPLOYED IN THE CHARACTERIZATION OF A PALMAR FINGERTIP. THE ACRONYMS SC, SG, SS, SB, PD AND RD REFER TO THE SKIN LAYERS CONSIDERED BY HyLioS: STRATUM CORNEUM, STRATUM GRANULOSUM, STRATUM SPINOSUM, STRATUM BASALE, PAPILLARY DERMIS AND RETICULAR DERMIS, RESPECTIVELY.

| Parameter                                   | Value              | Ref. |
|---|--------------------|------|
| Aspect Ratio of Skin Surface Folds          | 0.1                | [18] |
| SC Thickness (cm)                           | 0.013              | [18] |
| SG Thickness (cm)                           | 0.0123             | [31] |
| SS Thickness (cm)                           | 0.0123             | [31] |
| SB Thickness (cm)                           | 0.0123             | [31] |
| PD Thickness (cm)                           | 0.02               | [32] |
| RD Thickness (cm)                           | 0.2                | [33] |
| SC Melanosme Content (%)                    | 0.0                | [18] |
| SG Melanosme Content (%)                    | 0.0                | [18] |
| SS Melanosme Content (%)                    | 0.0                | [18] |
| SB Melanosme Content (%)                    | 0.15               | [18] |
| SC Colloidal Melanin Content (%)            | 0.06               | [18] |
| SG Colloidal Melanin Content (%)            | 0.06               | [18] |
| SS Colloidal Melanin Content (%)            | 0.06               | [18] |
| SB Colloidal Melanin Content (%)            | 0.06               | [18] |
| SB Melanosome Dim. ( $\mu m \times \mu m$ ) | $0.41 \times 0.17$ | [34] |
| Melanosme Eumelanin Conc. (g/L)             | 32.0               | [18] |
| Melanosme Pheomelanin Conc. (g/L)           | 2.0                | [18] |
| PD Blood Content (%)                        | 0.5                | [30] |
| RD Blood Content (%)                        | 2.0                | [35] |
| Dermal Oxyhemoglobin Fraction (%)           | 90.0               | [36] |
| Functional Hemoglobin Conc. in Blood (g/L)  | 147.0              | [37] |
| MetHb Conc. in Blood (g/L)                  | 1.5                | [6]  |
| CarboxyHb Conc. in Blood (g/L)              | 1.5                | [6]  |
| SulfHb Conc. in Blood (g/L)                 | 0.0                | [6]  |
| Blood Bilirubin Conc. (g/L)                 | 0.003              | [38] |
| SC Beta-carotene Conc. (g/L)                | $2.1E-4$           | [39] |
| Epidermis Beta-carotene Conc. (g/L)         | $2.1E-4$           | [39] |
| Blood Beta-carotene Conc. (g/L)             | $7.0E-5$           | [39] |
| SC Water Content (%)                        | 35.0               | [18] |
| Epidermis Water Content (%)                 | 60.0               | [18] |
| PD Water Content (%)                        | 75.0               | [18] |
| RD Water Content (%)                        | 75.0               | [18] |
| SC Lipid Content (%)                        | 20.0               | [40] |
| Epidermis Lipid Content (%)                 | 15.1               | [18] |
| PD Lipid Content (%)                        | 17.33              | [18] |
| RD Lipid Content (%)                        | 17.33              | [18] |
| SC Keratin Content (%)                      | 65.0               | [18] |
| SC Urocanic Acid Density (mol/L)            | 0.01               | [41] |
| Skin DNA Density (g/L)                      | 0.185              | [18] |
| SC Refractive Index                         | 1.55               | [18] |
| Epidermis Refractive Index                  | 1.4                | [18] |
| PD Refractive Index                         | 1.39               | [18] |
| RD Refractive Index                         | 1.41               | [18] |
| Melanin Refractive Index                    | 1.7                | [42] |
| PD Scatterers Refractive Index              | 1.5                | [43] |
| Radius of PD Scatterers (nm)                | 40.0               | [44] |
| PD Fraction Occupied by Scatterers (%)      | 22.0               | [13] |

papillary dermis. More specifically, we have deactivated the procedure used by HyLioS to account for this phenomenon. We note that this procedure is controlled by the Rayleigh scattering coefficient [14], [20], which is expressed as:

$$\mu_s^R(\lambda) = \frac{32\pi^4 r^3 v_f}{\lambda^4} \left( \frac{\eta^2 - 1}{\eta^2 + 1} \right)^2, \quad (1)$$

where  $r$  and  $v_f$  represent the radius and the volume fraction occupied by the scatterers (collagen fibrils), respectively, and  $\eta$  corresponds to the ratio between the refractive index of these scatterers ( $\eta_s$ ) and the refractive index of papillary dermis ( $\eta_{pd}$ ). Hence, to deactivate the Rayleigh scattering

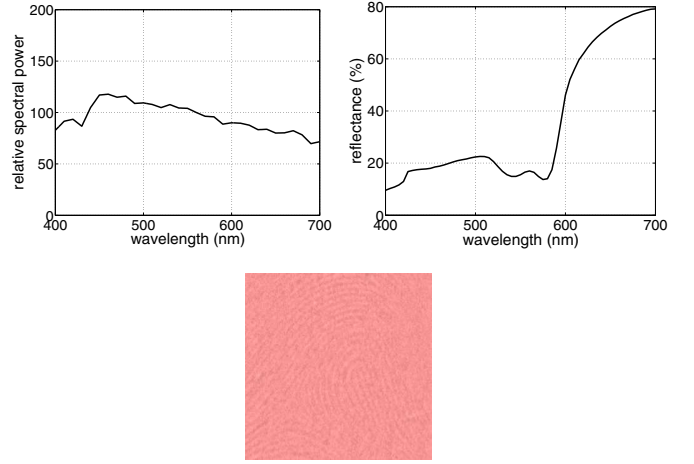


Fig. 3. Components of a convolution process employed to generate a skin swatch for a palmar fingertip in its normal (baseline) state characterized by the parameter values depicted in Table I. Top left: relative spectral power distribution of the CIE standard D65 illuminant. Top right: baseline reflectance curve: Bottom: resulting swatch.

in our simulations, we simply set  $\eta_f$  equal to  $\eta_{pd}$ , whose default value is provided in Table I.

We also generated skin swatches to complement our analyses. Their chromatic attributes were obtained from the convolution of a selected illuminant's relative spectral power distribution, the modeled reflectance data and the broad spectral response of the human photoreceptors [45]. This last step was performed by employing a standard XYZ to sRGB conversion procedure [46] and considering three CIE standard illuminants, namely D65, D50 and A [45]. Since the resulting qualitative observations remained unchanged regardless of which one we used, to conserve space, we elected to present in this paper the swatches generated using the D65 illuminant (daylight). Its relative spectral power distribution is depicted in Fig. 3 (top left). For comparison purposes, the skin swatch obtained using the baseline reflectance curve computed for the selected specimen is presented in Fig. 3 (bottom).

### III. RESULTS AND DISCUSSION

Initially, we bring to the reader's attention the presence of the characteristic "W" signature in the baseline reflectance curve depicted in Fig. 3 (top right), more specifically in the "green" region (500 to 600 nm) of the visible spectrum. The results of our first set of experiments depicted in Fig. 4 show that this signature, which is associated with the absorption spectrum of oxyhemoglobin (Fig. 2 (left)), vanishes with the reduction of this pigment's presence in the dermal tissues.

More revealingly, the results depicted in Fig. 4 also show that an increase in the values assigned to the target physiological parameters  $f_{deoxy}$  and  $v_{blood}^{rd}$  leads to a substantial reduction in the reflectance obtained in the "red" end (600 to 700 nm) of the visible spectrum, henceforth referred to as  $\rho_{red}$ . In contrast, one can observe much smaller changes in the reflectance obtained in the blue end of the visible spectrum, henceforth referred to as  $\rho_{blue}$ .

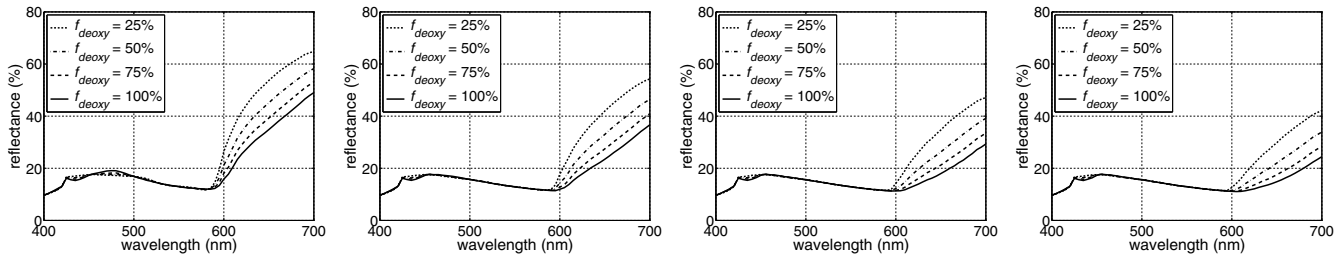


Fig. 4. Graphs depicting reflectance curves computed for a palmar fingertip considering variations on  $f_{deoxy}$ . From left to right, each set of curves was obtained considering  $v_{blood}^{r,d}$  equal to 5%, 10%, 15% and 20%, respectively.

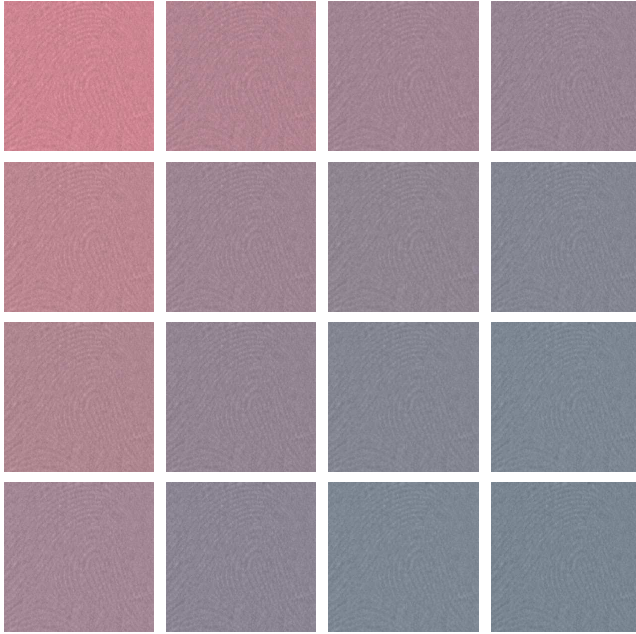


Fig. 5. Skin swatches obtained using the reflectance curves provided in Fig. 4. From top to bottom rows,  $f_{deoxy}$  varies from 25%, 50%, 75% and 100%, respectively. From left to right columns,  $v_{blood}^{r,d}$  varies from 5%, 10%, 15% and 20%, respectively.

These changes in  $\rho_{blue}$  and  $\rho_{red}$  are associated with the absorption spectra of deoxyhemoglobin (Fig. 2 (left)). Since this substance is a strong absorber at the blue end of the visible spectrum, light absorption rapidly reaches a limiting value in this spectral region as its presence in the dermal tissues increases. On the other hand, due to its relatively weak absorption capability in the red end, an increase in its presence results in a steady decrease in reflectance in this spectral region.

As it can be noted in the skin swatches depicted in Fig. 5, an increase in  $f_{deoxy}$  (leftmost column) or in  $v_{blood}^{r,d}$  (top row) results in a similar transition to a more accentuated purple hue, with a slightly stronger trend being observed with respect to  $v_{blood}^{r,d}$ . The combined effect of these variations (main diagonal), however, leads to a stronger bluish hue.

At a first glance, one might conclude that the manifestation of cyanotic chromatic attributes can be explained solely by the substantial decrease observed in  $\rho_{red}$  values. However,

$\rho_{blue}$  values, albeit having a relative low magnitude, are essential for eliciting the typical purple and blue hues associated with peripheral cyanosis. We believe that a significant portion of the light remission responses contributing to these values can be attributed to the Rayleigh scattering occurring within the papillary dermis [13], [20]. In order to demonstrate this aspect, we performed a second set of experiments in which the simulations were repeated while Rayleigh scattering was deactivated.

As indicated in the graphs presented in Fig. 6, the  $\rho_{blue}$  values become substantially smaller when Rayleigh scattering is not accounted for. For example, while  $\rho_{blue}$  at 450nm varies from 0.1753 (with  $f_{deoxy} = 25\%$  and  $v_{blood}^{r,d} = 5\%$ ) to 0.1736 (with  $f_{deoxy} = 100\%$  and  $v_{blood}^{r,d} = 20\%$ ) when the Rayleigh scattering is activated (Fig. 4), it varies from 0.0491 to 0.0488 under the same conditions when the Rayleigh scattering is deactivated (Fig. 6).

As a direct consequence of the substantial increase in the  $\rho_{red}$  values and the subtle reduction in the already relatively low  $\rho_{blue}$  values, the perceived coloration of the palmar fingertip site changes from red to dark red when the Rayleigh scattering is deactivated. This chromatic transition, depicted in Fig. 7, is consistent with the perceived colorations of oxygenated and deoxygenated blood respectively [11], [12], which are predominantly determined by the strong light absorption behaviour of the hemoglobins in the blue end of the visible spectrum (Fig. 2 (left)).

Finally, it is worth noting that the observations derived from our *in silico* experiments may be applicable to an old, albeit still not fully answered question: ‘‘Why do veins appear blue when venous blood has a dark red color?’’ The reason for the bluish color of veins had been attributed not to larger  $\rho_{blue}$  values, but rather to a decrease in the  $\rho_{red}$  values [11]. We believe that, like the cyanosis case, a significant portion to the light remission responses contributing to  $\rho_{blue}$  values results from Rayleigh scattering. This phenomenon reduces the probability of light travelling at lower wavelengths to reach the vein where it might be susceptible to absorption by the relative larger amount of deoxyhemoglobin (when compared to the neighbour skin sites) present in the circulating blood. We remark that light traveling at longer wavelengths is considerably less affected by this type of scattering [14]. Hence, it is more likely to penetrate deeper and reach the venous blood, where it might

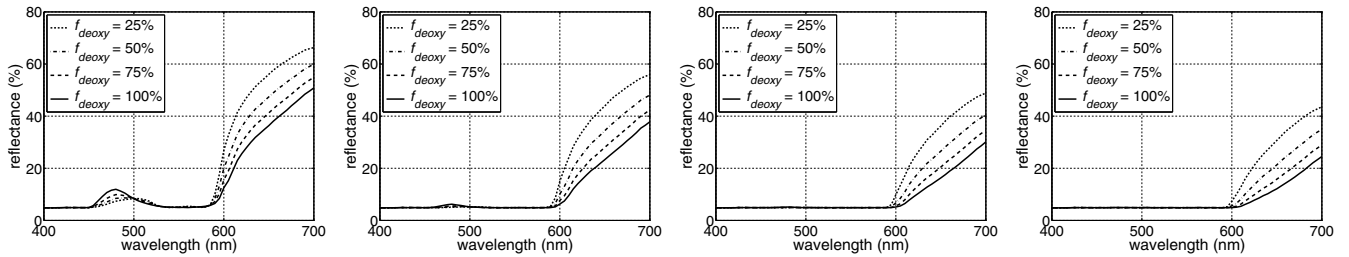


Fig. 6. Graphs depicting reflectance curves computed for a palmar fingertip considering variations on  $f_{deoxy}$  and the deactivation of Rayleigh scattering within the papillary dermis. From left to right, each set of curves was obtained considering  $v_{blood}^r$  equal to 5%, 10%, 15% and 20%, respectively.

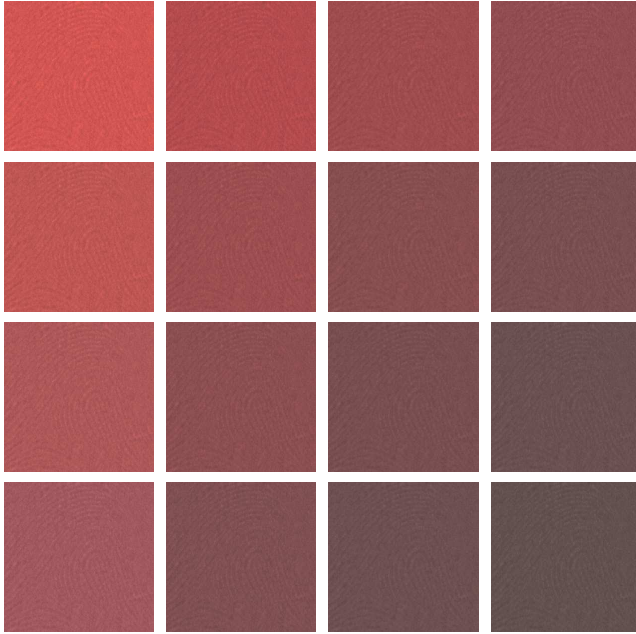


Fig. 7. Skin swatches obtained using the reflectance curves provided in Fig. 6. From top to bottom rows,  $f_{deoxy}$  varies from 25%, 50%, 75% and 100%, respectively. From left to right columns,  $v_{blood}^r$  varies from 5%, 10%, 15% and 20%, respectively.

be absorbed, consequently reducing the  $\rho_{red}$  values.

#### IV. CONCLUSION AND FUTURE WORK

In this paper, we have investigated the impact of variations in key physiological parameters on the biophysical processes leading to the chromatic attributes of peripheral cyanosis. Our findings indicate that, although an increase in either the deoxyhemoglobin amount or in the reticular dermis blood content can result in a cyanotic purple hue as previously reported in the literature, it is their combined effect that can lead to a more characteristic cyanotic bluish hue.

Our findings also show that, although these chromatic transitions are directly associated with a reduction in the  $\rho_{red}$  values, the contribution provided by the  $\rho_{blue}$  values is essential for eliciting these transitions. Moreover, the results of our experiments indicate that a significant portion of this contribution can be attributed to Rayleigh scattering occurring within the papillary dermis.

Although the putative occurrence of Rayleigh scattering within the dermal tissues has been discussed before (e.g., [47]), to the best of our knowledge, this is the first time that a direct connection between cyanotic chromatic attributes and Rayleigh scattering occurring within the papillary dermis is examined in the scientific literature. It is worth highlighting that the assessment of this hypothesis was made possible through *in silico* experiments.

Recall that it would be extremely difficult to obtain *in situ* Rayleigh scattering profiles within a thin skin layer like the papillary dermis using existing “wet” lab technologies. Moreover, assuming that it would be possible to separate this layer from a donated skin specimen, the dermal blood content would differ from the one observed under *in vivo* conditions. Incidentally, these aspects may explain, at least partially, why such measurements are not available in the literature. Hence, in a broader scientific context, the predictive investigation framework employed in this research can be viewed as a “computational probe” that provides unique insights into biophysical phenomena taking place inside living human skin tissues. Further developments on this topic will likely require the pairing of these insights with new data obtained through traditional experimental techniques.

We remark that peripheral cyanosis can also be evoked by an abnormal presence of methemoglobin or sulfhemoglobin in the dermal tissues [3], [4]. Since these substances are also characterized by a strong absorption behaviour in the blue end of the visible spectrum and a weak behaviour in the red end [6], peripheral cyanotic chromatic attributes triggered by them are also affected by the same light attenuation phenomena discussed in this paper. Hence, as the presence of dysfunctional hemoglobins in the dermal tissues increases, the resulting changes in the cyanotic chromatic attributes are likely to follow these same patterns observed with respect to the increase in the presence of deoxyhemoglobin. As future work, we intend to investigate the validity of this assumption.

Cyanosis can be observed in individuals at different growth stages, from adults to infants [9]. Since these individuals are characterized by distinct morphological characteristics, we also intend to investigate the impact of variations on morphological parameters, such as the thickness of the papillary dermis and the radius of the fibrils found in this tissue, on hyperspectral responses associated with both types of cyanosis, peripheral and central.

## REFERENCES

- [1] C.D. Marple, "Cyanosis," *The American Journal of Nursing*, vol. 58, no. 2, pp. 222–235, 1958.
- [2] G. Casey, "Oxygen transport and the use of pulse oxymetry," *Nursing Standard*, vol. 15, no. 47, pp. 46–53, 2001.
- [3] A. Baernstein, K.M. Smith, and J.G. Elmore, "Singing the blues: is it really cyanosis?," *Resp. Care*, vol. 53, no. 8, pp. 1081–1084, 2008.
- [4] S.M. McMullen and W. Patrick, "Cyanosis," *The American Journal of Medicine*, vol. 126, no. 3, pp. 210–212, 2013.
- [5] C. Smollin and K. Olson, "Carbon monoxide poisoning (acute)," *BMJ Clinical Evidence*, vol. 2103, pp. 1–12, 2008.
- [6] G.V.G. Baranoski, T.F. Chen, B.W. Kimmel, E. Miranda, and D. Yim, "On the noninvasive optical monitoring and differentiation of methemoglobinemia and sulfhemoglobinemia," *J. Biomed. Opt.*, vol. 17, no. 9, pp. 097005–1–14, 2012.
- [7] S. Goldschmidt and A. B. Light, "A cyanosis, unrelated to oxygen unsaturation, produced by increased peripheral venous pressure," *Am. J. Physiol.*, vol. 73, pp. 173–192, 1925.
- [8] C. Lundsgaard and D. Van Slyke, "Cyanosis," *Medicine*, vol. II, pp. 1–76, 1923.
- [9] R.P. Smith, "The blue baby syndromes," *American Scientist*, vol. 97, no. 2, pp. 94–96, 2009.
- [10] N.F. Azmi, F. Delbressine, and L. Feijs, "Conceptual determination and assessment of cyanosis," *Int. J. Bioscience, Biochemistry and Bioinformatics*, vol. 6, no. 3, pp. 75–83, 2016.
- [11] A. Kienle, L. Lilge, A. Vitkin, M.S. Patterson, B.C. Wilson, R. Hibst, and R. Steiner, "Why do veins appear blue? A new look at an old question," *Applied Optics*, vol. 35, no. 7, pp. 1151–1160, 1996.
- [12] D. Yim, G.V.G. Baranoski, B.W. Kimmel, T.F. Chen, and E. Miranda, "A cell-based light interaction model for human blood," *Computer Graphics Forum*, vol. 31, no. 2, pp. 845–854, 2012.
- [13] S.L. Jacques, "Origins of tissue optical properties in the UVA, visible, and NIR regions," *OSA TOPS on Adv. in Opt. Imaging and Photon Migration*, vol. 2, pp. 364–369, 1996.
- [14] E.J. McCartney, *Optics of the atmosphere: Scattering by molecules and particles*, John Wiley & Sons, 1976.
- [15] S.A. Prahl, "Optical absorption of hemoglobin," Tech. Rep., Oregon Medical Laser Center, 1999.
- [16] S.L. Jacques, "Optical absorption of melanin," Tech. Rep., Oregon Medical Laser Center, 2001.
- [17] B.D. Ventura, C. Lemerle, K. Michalodimitrakis, and L. Serrano, "From *in vivo* to *in silico* biology and back," *Nature*, vol. 443, pp. 527–553, 2006.
- [18] G.V.G. Baranoski, A. Dey, and T.F. Chen, "Assessing the sensitivity of human skin hyperspectral responses to increasing anemia severity levels," *J. Biomed. Opt.*, vol. 9, no. 20, pp. 095002–1–14, 2015.
- [19] G.V.G. Baranoski and M.W.Y. Lam, "Qualitative assessment of undetectable melanin distribution in lightly pigmented irides," *J. Biomed. Opt.*, vol. 12, no. 3, pp. (030501):1–3, August 2007.
- [20] T.F. Chen, G.V.G. Baranoski, B.W. Kimmel, and E. Miranda, "Hyperspectral modeling of skin appearance," *ACM Trans. Graph.*, vol. 34, no. 3, pp. 31:1–14, 2015.
- [21] G.V.G. Baranoski and T.F. Chen, "On the identification and interpretation of human skin spectral responses under adverse environmental conditions," in *37th Annual International Conference of the IEEE Engineering in Medicine and Biology Society (EMBC)*, Milan, Italy, August 2015, pp. 845–848.
- [22] T.F. Chen and G.V.G. Baranoski, "Melanosome distribution patterns affecting skin reflectance: Implications for the *in vivo* estimation of epidermal melanin content," in *37th Annual International Conference of the IEEE Engineering in Medicine and Biology Society (EMBC)*, Milan, Italy, August 2015, pp. 4415–4418.
- [23] T.F. Chen and G.V.G. Baranoski, "Effective compression and reconstruction of human skin hyperspectral reflectance databases," in *37th Annual International Conference of the IEEE Engineering in Medicine and Biology Society (EMBC)*, Milan, Italy, August 2015, pp. 7027–7030.
- [24] G.V.G. Baranoski, J.G. Rokne, and G. Xu, "Virtual spectrophotometric measurements for biologically and physically-based rendering," *The Visual Computer*, vol. 17, no. 8, pp. 506–518, 2001.
- [25] Natural Phenomena Simulation Group (NPSG), *Run HyLloS Online*, School of Computer Science, University of Waterloo, Ontario, Canada, 2017, <http://www.npsg.uwaterloo.ca/models/hyliosEx.php>.
- [26] G.V.G. Baranoski, T. Dimson, T. F. Chen, B. Kimmel, D. Yim, and E. Miranda, "Rapid dissemination of light transport models on the web," *IEEE Comput. Graph.*, vol. 32, pp. 10–15, 2012.
- [27] NPSG, *Human Skin Data*, Natural Phenomena Simulation Group (NPSG), School of Computer Science, University of Waterloo, Ontario, Canada, 2014, <http://www.npsg.uwaterloo.ca/data/skin.php>.
- [28] Y. Yamaguchi, S. Itami, H. Watabe, K. Yasumoto, Z. A. Abdel-Malek, T. Kubo, F. Rouzaud, A. Tanemura, K. Yoshikawa, and V.J. Hearing, "Mesenchymal-epithelial interactions in the skin: increased expression of dickkopf1 by palmo-plantar fibroblast inhibits melanocyte growth and differentiation," *J. Cell Biol.*, vol. 165, no. 2, pp. 275–285, 2004.
- [29] R.H. Turner, G.E. Burch, and W.A. Sodeman, "Studies in the physiology of blood vessels in man. III. Some effects of raising and lowering the arm upon the pulse volume and blood volume of the human finger tip in health and in certain diseases of the blood vessels," *J. Clin. Invest.*, vol. 16, no. 5, pp. 789–798, 1937.
- [30] A. Caduff, M.S. Talary, and P. Zakharov, "Cutaneous blood perfusion as a perturbing factor for noninvasive glucose monitoring," *Diabetes Technology & Therapeutics*, vol. 12, no. 1, pp. 1–9, 2010.
- [31] J.T. Whitton and J.D. Everall, "The thickness of the epidermis," *British Journal of Dermatology*, vol. 89, pp. 467–476, 1973.
- [32] M. Schwarz, M. Omar, A. Buehler, J. Aguirre, and V. Ntziachristos, "Implications of ultrasound frequency in optoacoustic mesoscopy of the skin," *IEEE Trans. Med. Imaging*, vol. 34, no. 2, pp. 672–677, 2015.
- [33] R.R. Anderson and J.A. Parrish, "The optics of human skin," *J. Invest. Dermatol.*, vol. 77, no. 1, pp. 13–9, 1981.
- [34] R.L. Olson, J. Gaylor, and M.A. Everett, "Skin color, melanin, and erythema," *Arch. Dermatol.*, vol. 108, no. 4, pp. 541–544, 1973.
- [35] G.E. Nilsson, T. Tenland, and P.A. Öberg, "Evaluation of a laser Doppler flowmeter for measuring of tissue blood flow," *IEEE Transactions on Biomedical Engineering*, vol. 27, no. 10, pp. 597–604, 1980.
- [36] M.L. Noll and J.F. Byers, "Usefulness of measures of  $S_{vo2}$ ,  $S_{po2}$ , vital signs, and derived dual oximetry parameters as indicators of arterial blood gas variables during weaning of cardiac surgery patients from mechanical ventilation," *Heart & Lung*, vol. 24, no. 3, pp. 220–227, 1995.
- [37] A.N. Yaroslavsky, A.V. Priezhev, J. Rodrigues, I.V. Yaroslavsky, and H. Battarbee, "Optics of blood," in *Handbook of Optical Biomedical Engineering*, V.V. Tuchin, Ed., Bellingham, USA, 2002, pp. 169–216, SPIE-Press.
- [38] S.D. Zucker, P.S. Horn, and K.E. Sherman, "Serum bilirubin levels in the US population: Gender effect and inverse correlation with colorectal cancer," *Hepatology*, vol. 40, no. 4, pp. 827–835, 2004.
- [39] R. Lee, M. M. Mathews-Roth, M. A. Pathak, and J. A. Parrish, "The detection of carotenoid pigments in human skin," *J. Invest. Dermatol.*, vol. 64, no. 3, pp. 175–177, 1975.
- [40] M.L. Williams, M. Hincenbergs, and K.A. Holbrook, "Skin lipid content during early fetal development," *J. Invest. Dermatol.*, vol. 91, no. 3, pp. 263–268, 09 1988.
- [41] A. R. Young, "Chromophores in human skin," *Phys. Med. Biol.*, vol. 42, no. 5, pp. 789, 1997.
- [42] A.N. Bashkatov, E.A. Genina, V.I. Kochubey, M.M. Stolnitz, T.A. Bashkatova, O.V. Novikova, A.Y. Peshkova, and V.V. Tuchin, "Optical properties of melanin in the skin and skin-like phantoms," in *SPIE Vol. 4162, Controlling Tissue Optical Properties: Applications in Clinical Study*, V.V. Tuchin, Ed.
- [43] X. Wang, T.E. Milner, and M.C. Chang and J.S. Nelson, "Group refractive index measurement of dry and hydrated type I collagen films using optical low-coherence reflectometry," *J. Biomed. Opt.*, vol. 12, pp. 212–216, 1996.
- [44] H. Arao, M. Obata, T. Shimada, and S. Hagsisawa, "Morphological characteristics of the dermal papillae in the development of pressure sores," *Journal of Tissues Viability*, vol. 8, no. 3, pp. 17–23, 1998.
- [45] R.W.G. Hunt, *Measuring Colour*, Ellis Horwood Limited, Chichester, England, 2nd edition, 1991.
- [46] G.V.G. Baranoski and A. Krishnaswamy, *Light & Skin Interactions: Simulations for Computer Graphics Applications*, Morgan Kaufmann/Elsevier, Burlington, MA, USA, 2010.
- [47] E.A. Edwards and S.Q. Duntley, "The pigments and the color of living human skin," *The American Journal of Anatomy*, vol. 65, no. 1, pp. 1–33, 1939.